Accurate Current Sharing and PCC Voltage Restoration in LVDC Microgrid without Communication Network

Khanh Duc Hoang
School of Electrical Engineering
University of Ulsan
Ulsan, Korea
E-mail: duckhanhht13989@gmail.com

Dong-Choon Lee
Department of Electrical Engineering
Yeungnam University
Gyeongsan, Korea
E-mail: dclee@yu.ac.kr

Hong-Hee Lee
School of Electrical Engineering
University of Ulsan
Ulsan, Korea
E-mail: hhlee@mail.ulsan.ac.kr

***Abstract*— In this paper, a control strategy is proposed for both accurate current sharing among distributed generators (DGs) and the point of common coupling (PCC) voltage restoration in low voltage direct current (LVDC) microgrid by injecting a small AC signal to the output voltage of the DG. The small AC signal frequency changes proportionally to the per unit (pu) output current of the corresponding DG, and the DG output voltage is regulated to share every DG with the equivalent frequency in the steady state. Especially, for easy implementation, the reactive power of the AC signal is controlled to indirectly regulate the AC signal frequency. Moreover, the equivalent pu output current is used to determine the voltage shift-up in order to restore the PCC voltage. Because the proposed control scheme is developed with the fully distributed manner at local controller for each DG, it can be implemented economically without external communication network. The effectiveness of the proposed control method is proved by the simulation.**

***Index Terms*—DC microgrid, droop control, current sharing, voltage improvement.**

I. INTRODUCTION

With the substantial penetration of the renewable energy source that has a dc output power (e.g., photovoltaics (PVs), fuel cells) into power system and the growing of DC load applications, DC microgrid has been attracting many interests. The main motivations to develop DC microgrid are its highly efficient energy conversion and simple control scheme [1]–[3]. In order to effectively manage power systems in DC microgrids, it is important to ensure the stable operation and cooperation of different types of energy sources.

In [4] and [5], the master-slave control methods were presented to cooperate among the distributed generators (DGs) in DC microgrids where a high bandwidth communication were used to share the information among the DGs. However, these approaches raise the risk of the single point failure which damages the system operation. Another approach is the voltage droop control to properly control the load sharing among the DGs [6], [7]. In this approach, the line resistances are neglected to make the output voltages stable. However, the accurate current sharing is deteriorated due to the actual line resistances. In addition, the voltage drop due to the inherent characteristic of voltage droop control reduces the voltage on the point of common coupling (PCC) in DC microgrid [8]. In order to improve the current sharing accuracy and the voltage regulation in DC microgrid, the secondary control layers relying on communication network were proposed [9]–[12]. However, the communication delay affects the stability and the reliability of the system especially when the sources are separated with long feeders [13].

With the attempt to be independent on the communication network, authors in [14] proposed "Power Talk" concept to communicate among the DGs. In this method, high frequency communication signal is modulated to the output power of the corresponding DG, and the electric lines are used as communication links. However, this approach leans on the states of the system such as the line resistance and the load condition which are unpredictable in practical application. Meanwhile, the frequency-based power sharing technique was firstly developed for AC power systems [15], and then, it was also applied to the DC microgrid [16]. However, the method are not suitable for the low voltage DC (LVDC) microgrids with the resistive line characteristics [17]. Based on the method proposed in [15] and [16], the frequency-based current sharing technique applied to LVDC microgrids was proposed in [17]–[19]. However, in [17] and [19], only accurate current sharing is achieved, while the PCC voltage drop is not considered. In [18], the PCC voltage restoration at distributed secondary layer was taken into account along with an accurate current sharing. Nonetheless, the control scheme is very complicated due to the secondary control was not decoupled with the primary control.

In this paper, we propose an accurate current sharing and the PCC voltage restoration in LVDC microgrid based on the frequency-based current sharing technique. In the proposed control method, a small AC signal with the frequency generated according to the per unit (pu) output current is injected to the output voltage of the corresponding DG. In the steady state, the accurate current sharing is achieved by regulating the injected AC signal frequency to be equivalent frequency. And also, the equivalent pu output current is used to restore the PCC voltage. Furthermore, the controller only uses the local information about the output voltages and current of DGs without external communication network, which enables the system economic and easy to implement. The proposed control method is analyzed theoretically, and its effectiveness is also verified by simulation.

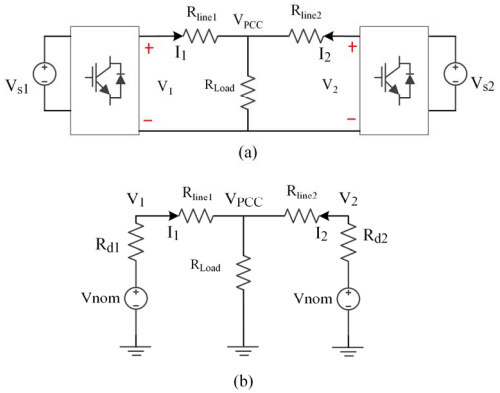

Fig. 1. DC microgrid: a) Two source DC microgrid model, b) Equivalent circuit

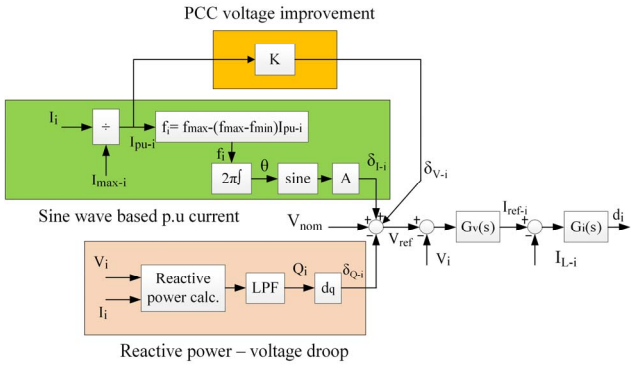

Fig. 2. Proposed control scheme

II. Conventional Droop Control

For simple analysis, a DC microgrid model with two DGs is considered as shown in Fig. 1(a), and its corresponding equivalent circuit is shown in Fig. 1(b). In Fig. 1, $\{V_1, I_1, R_1\}$ and $\{V_2, I_2, R_2\}$ are the output voltage, output current and droop coefficient of DG 1 and DG 2, respectively, V_{nom} is the nominal voltage, and R_{load}, R_{line1}, R_{line2} are the equivalent load resistance and line resistance of DG 1 and DG 2. According to Fig. 1(b), the output voltage of two DGs is determined by the droop control:

$$V_i = V_{nom} - R_i I_i, i = 1,2 \tag{1}$$

And, the PCC voltage (V_{PCC}) is calculated from Fig. 2:

$$V_{PCC} = V_{nom} - R_{d1} I_1 - R_{line1} I_1;\ V_{PCC} = V_{nom} - R_{d2} I_2 - R_{line2} I_2 \tag{2}$$

From (2), the output current ratio between two DGs is obtained:

$$\frac{I_1}{I_2} = \frac{R_{d2}}{R_{d1}} + \frac{R_{line2} - R_{d2}\dfrac{R_{line1}}{R_{d1}}}{R_{d1} + R_{line1}} \tag{3}$$

From (3), in order to guarantee the accurate current sharing among the DGs, the following constraint should be satisfied:

$$\frac{R_{d1}}{R_{line1}} = \frac{R_{d2}}{R_{line2}} \tag{4}$$

In the practical system, the condition (4) is difficult to obtain because of different line resistances.

Furthermore, the voltage on PCC in (2) is normally lower than the nominal value because of the effects of the voltage droop control and line resistances.

III. Principle of The Proposed Control Method

A. Frequency-based accurate current sharing

In order to solve the inaccurate current sharing problem, an accurate current sharing method is proposed by utilizing a small AC signal frequency which changes according to the pu current of the corresponding DG. The corresponding control scheme of the two DGs in Fig. 1(a) are presented in Fig. 2. The small AC signal ($\delta_{I\text{-}i} = A\sin(2\pi f_i t)$) with the amplitude and the frequency denoted as A and f_i, respectively, is injected to the output voltage. The frequency of the injected AC signal at the *i-th* DG is defined as following:

$$f_i = f_{\max} - (f_{\max} - f_{\min}) I_{pu-i};\quad I_{pu-i} = \frac{I_i}{I_{\max-i}}, \tag{5}$$

where f_{max} and f_{min} are the maximum and minimum frequency of the AC signal injected to the *i-th* DG, I_i, $I_{max\text{-}i}$ and $I_{pu\text{-}i}$ are the output current, current rating and pu current of the *i-th* DG, respectively.

Then, the corresponding phase angle of the injected AC signal (θ_i) at the *i-th* DG becomes from (5):

$$\theta_i = 2\pi f_i t = 2\pi\left[f_{\max} - (f_{\max} - f_{\min}) I_{pu-i}\right] t \tag{6}$$

From (5) and (6), in order to achieve the accurate current sharing, the frequency of each AC signal should be equal. For example, in Fig. 1 which includes 2 DGs, the phase angle difference between the two AC signals at the two DGs becomes zero when the pu currents I_{pu-1} and I_{pu-2} have same value, which means the accurate current sharing, i.e.,

$$\theta = \theta_1 - \theta_2 = 2\pi(f_1 - f_2)t = 2\pi(f_{\max} - f_{\min})(I_{pu-2} - I_{pu-1})t = 0$$
$$\text{when } I_{pu-1} = I_{pu-2}\ . \tag{7}$$

If there exists the phase difference in (7), a small reactive power flows in the microgrid corresponding to the injected AC signal frequency [20]. The reactive power flows only through the DGs because the load impedance is generally higher than the line impedances, and it is calculated from Fig. 1(b) by inserting the AC signals instead of the DC voltages:

$$Q_1 = -\frac{A^2}{2(R_{line1} + R_{line2})}\sin\theta$$
$$Q_2 = \frac{A^2}{2(R_{line1} + R_{line2})}\sin\theta \tag{8}$$

where Q_i (i=1,2) is the reactive power generated from the injected small AC signal of the *i-th* DG.

As shown in (8), because the reactive power contains the information about the phase difference of two AC signals, the reactive power flow in the grid can be regulated to indirectly keep the zero phase difference instead of the AC signal frequency.

TABLE I

NOMINAL PARAMETER OF CONVERTER

Parameter	Symbol	Value
Input voltage	V_S	60V
Output voltage	V_{out}	100V
Inductor	L	0.5mH
Capacitor	C	2200μF
Resistive load	R_{load}	20Ω
Current controller	$G_{PI\text{-}i}(s)$	0.5+30/s
Voltage controller	$G_{PI\text{-}v}(s)$	0.5+8/s

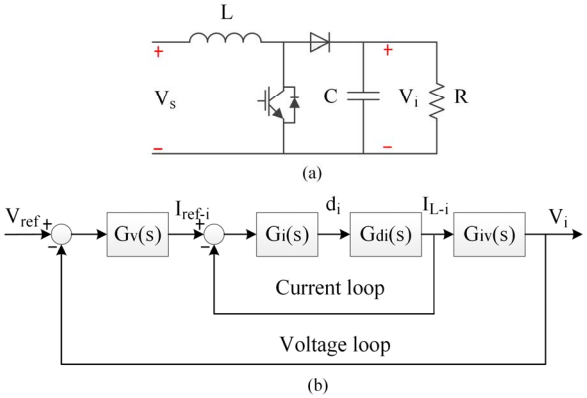

Fig. 3. Boost converter topology and control loops: a) Boost converter, b) Voltage – Current control loop

In order to control the reactive power flow, a voltage-reactive power droop relationship is proposed as the following:

$$V_{ref-i} = V_{nom} + \delta_{I-i} - d_q Q_i G_{LPF}(s) \quad (9)$$

where d_q is the voltage-reactive power droop gain, G_{LPF} is the low pass filter transfer function to eliminate the high frequency components in the calculated reactive power.

As shown in Fig. 2, the injected AC signal frequency, which is proportional to the pu current, is regulated by adding the voltage-reactive power droop element to the reference voltage. When the reactive power becomes zero, the frequencies of all DGs become the same value, and the accurate current sharing is obtained.

Because the control signals in (9) can be obtained locally at each DG, the proposed control scheme can be implemented without communication network.

B. The PCC voltage restoration

In the steady state, when the proportional current sharing is achieved, the pu output currents of all DGs are equal. The pu current for DG changes with the load variation, and the PCC voltage also changes according to the pu current variation. Therefore, the pu output current can be used to adjust the DG output voltage reference without detecting the PCC voltage magnitude. In this paper, a voltage shift-up to restore the PCC voltage to nominal value is added to the reference voltage of each DG by using the pu output current, and the voltage shift-up value ($\delta_{V\text{-}i}$) is given as following:

$$\delta_{V-i} = K_V I_{pu-i} \ , \quad (10)$$

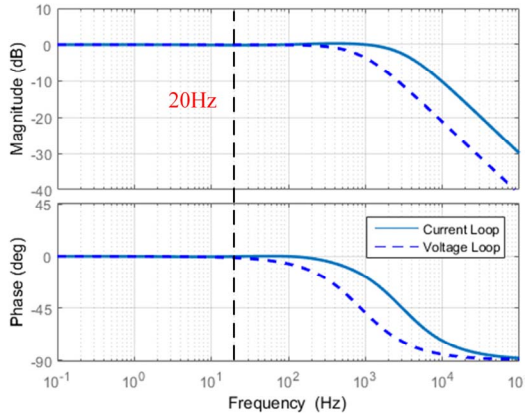

Fig. 4. Bode diagram of Voltage – Current closed loop

where K_V is the compensation gain for voltage restoration. Then, the reference voltage of the *i-th* DG ($V_{ref\text{-}i}$) in (9) is modified as following in order to restore the PCC voltage to nominal value as well as to achieve the proportional current sharing:

$$V_{ref-i} = V_{nom} + \delta_{I-i} - d_q Q_i G_{LPF}(s) + \delta_{V-i} \quad (11)$$

C. Selection of injected AC signal parameters

Fig. 3(a) shows the boost converter with the parameters presented in TABLE I as the interface converter for DG, and its control block diagram is shown in Fig. 3(b). In Fig. 3(b), $G_v(s)$ and $G_i(s)$ are the voltage and current Proportional-Integral (PI) controllers, $G_{di}(s)$ and $G_{iv}(s)$ are the transfer functions of the duty cycle to the inductor current and the inductor current to output voltage, respectively

In order to successfully track the injected AC signal merged into the DC voltage component through the PI controllers, the AC signal frequency should be smaller than the bandwidth of the voltage and current control loops. With the parameters presented in TABLE I, the closed loop transfer functions of the voltage and current control loops are obtained and their bode diagrams are plotted in Fig. 4. From Fig. 4, the injected AC signal frequency is chosen as 20 Hz to guarantee the tracking performance of the controllers.

Regarding to the amplitude of the injected AC signal, since there is no standard about the maximum ripple in LVDC microgrid, the amplitude is selected as small as possible to restrict the ripple of the DC voltage. However, it should be large enough to measure the signal amplitude. In this study, the amplitude of the injected AC signal is chosen as 1.0V (1% of V_{nom}).

IV. Stability Analysis

Considering the DC microgrid in Fig. 1(a), the output currents of the DGs can be calculated as follows:

$$\begin{aligned} I_1 &= \alpha_1 V_1 - \lambda V_2 \\ I_2 &= \alpha_2 V_2 - \lambda V_1 \end{aligned} \ , \quad (12)$$

where

TABLE II

SYSTEM PARAMETERS

Parameter	Symbol	Value
DG 1 current rating	I_{max-1}	15A
DG 2 current rating	I_{max-2}	10A
Maximum frequency	f_{max}	20Hz
Minimum frequency	f_{min}	19Hz
AC signal amplitude	A	1V
Droop gain	d_q	0.5
Voltage restoration gain	K_V	12
LPF cut off frequency	f_{LPF}	5Hz
Line resistance	R_{line1}, R_{line2}	1.5, 1.0Ω
Current controller	$G_{PI\text{-}i}(s)$	0.5+30/s
Voltage controller	$G_{PI\text{-}v}(s)$	0.5+8/s

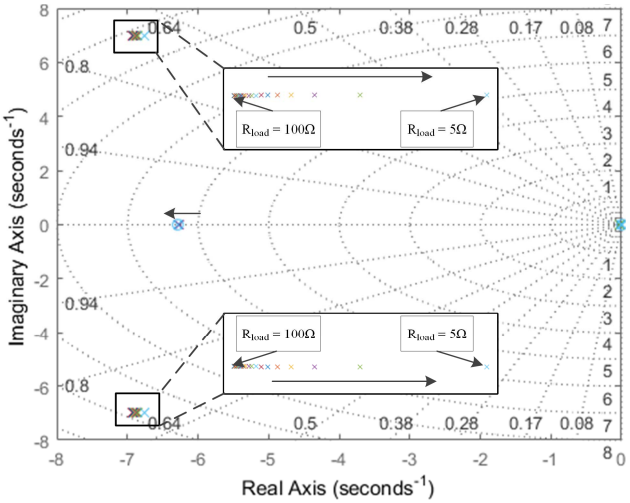

Fig. 5. Dominant poles for different load values (R_{load})

$$\alpha_1 = \frac{R_{line2}+R_{load}}{R_{line1}R_{line2}+R_{line1}R_{load}+R_{line2}R_{load}}$$
$$\alpha_2 = \frac{R_{line1}+R_{load}}{R_{line1}R_{line2}+R_{line1}R_{load}+R_{line2}R_{load}} \quad . \tag{13}$$
$$\lambda = \frac{R_{load}}{R_{line1}R_{line2}+R_{line1}R_{load}+R_{line2}R_{load}}$$

Substituting (12) into (5) and considering the small signals of the pu currents and injected AC signal frequencies,

$$\hat{I}_{pu-1} = \frac{\alpha_1\hat{V}_1 - \lambda\hat{V}_2}{I_{\max-1}}$$
$$\hat{I}_{pu-2} = \frac{\alpha_2\hat{V}_2 - \lambda\hat{V}_1}{I_{\max-2}} \tag{14}$$

$$\hat{f}_1 = -(f_{\max}-f_{\min})\frac{\alpha_1\hat{V}_1 - \lambda\hat{V}_2}{I_{\max-1}}$$
$$\hat{f}_2 = -(f_{\max}-f_{\min})\frac{\alpha_2\hat{V}_2 - \lambda\hat{V}_1}{I_{\max-2}} \tag{15}$$

Substituting (15) into (6) and (7), we can obtain the small signals of phase angles, the instantaneous AC signal values and the phase angle difference in the frequency domain:

$$\hat{\theta}_1 = -\frac{2\pi}{s}(f_{\max}-f_{\min})\frac{\alpha_1\hat{V}_1 - \lambda\hat{V}_2}{I_{\max-1}}$$
$$\hat{\theta}_2 = -\frac{2\pi}{s}(f_{\max}-f_{\min})\frac{\alpha_2\hat{V}_2 - \lambda\hat{V}_1}{I_{\max-2}} \tag{16}$$

$$\hat{\delta}_{I-1} = A\cos\theta_1 \times \hat{\theta}_1$$
$$\hat{\delta}_{I-2} = A\cos\theta_2 \times \hat{\theta}_2 \tag{17}$$

$$\hat{\theta} = \frac{2\pi}{s}(f_{\max}-f_{\min})\left(\frac{\alpha_2\hat{V}_2 - \lambda\hat{V}_1}{I_{\max-2}} - \frac{\alpha_1\hat{V}_1 - \lambda\hat{V}_2}{I_{\max-1}}\right) \tag{18}$$

From (8) and (18), the small signals of the reactive powers are

$$\hat{Q}_1 = -\frac{A^2}{2(R_{line1}+R_{line2})}\hat{\theta}$$
$$= -\frac{\pi(f_{\max}-f_{\min})A^2}{s(R_{line1}+R_{line2})}\left(\frac{\alpha_2\hat{V}_2 - \lambda\hat{V}_1}{I_{\max-2}} - \frac{\alpha_1\hat{V}_1 - \lambda\hat{V}_2}{I_{\max-1}}\right) \tag{19}$$
$$\hat{Q}_2 = \frac{A^2}{2(R_{line1}+R_{line2})}\hat{\theta}$$
$$= \frac{\pi(f_{\max}-f_{\min})A^2}{s(R_{line1}+R_{line2})}\left(\frac{\alpha_2\hat{V}_2 - \lambda\hat{V}_1}{I_{\max-2}} - \frac{\alpha_1\hat{V}_1 - \lambda\hat{V}_2}{I_{\max-1}}\right)$$

From (10) and (14), the small signal of voltage shift-up becomes

$$\hat{\delta}_{V-1} = K_V\hat{I}_{pu-1} = K_V\frac{\alpha_1\hat{V}_1 - \lambda\hat{V}_2}{I_{\max-1}}$$
$$\hat{\delta}_{V-2} = K_V\hat{I}_{pu-2} = K_V\frac{\alpha_2\hat{V}_2 - \lambda\hat{V}_1}{I_{\max-2}} \quad . \tag{20}$$

Meanwhile, the local voltage loop, G_V, can be derived from the local voltage and the current controllers [9]:

$$G_V = \frac{V_i}{V_{ref-i}} = \frac{G_{PI-v}G_{PI-i}}{1+G_{PI-v}G_{PI-c}i}, \ i=1,2 \tag{21}$$

By substituting (17), (19), (20) and (21) into (11), the small signal relationship between the *i-th* DG output voltage, V_i, and the nominal voltage, V_{nom}, is derived as a function of R_{load} :

$$\hat{V}_i = g_i\left(\hat{V}_{nom}, R_{load}\right), i=1,2 \tag{22}$$

By using m-script and symbolic toolboxes in MATLAB and the parameters in TABLE II, (22) can be solved.

Fig. 5 shows the positions of the system dominant poles when the load resistance changes from 100Ω to 5Ω. From Fig. 5, when the load resistance decreases, the dominant poles tend to move toward the right half plane, which means the system stability decreases. However, the poles still place in the left half plane, which proves the system stability.

V. SIMULATION RESULTS

In order to verify the effectiveness of the proposed control method, the DC microgrid including two DGs as shown in Fig. 6 is considered, and the parameters of the system are presented in TABLE II. The simulation is implemented in two cases: the conventional droop control and the proposed control scheme. In order to investigate the proposed PCC voltage restoration method, the load condition is changed by

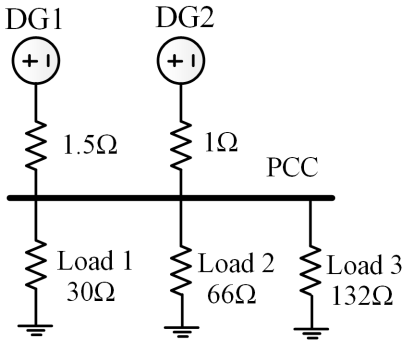

Fig. 6. DC microgrid in simulation

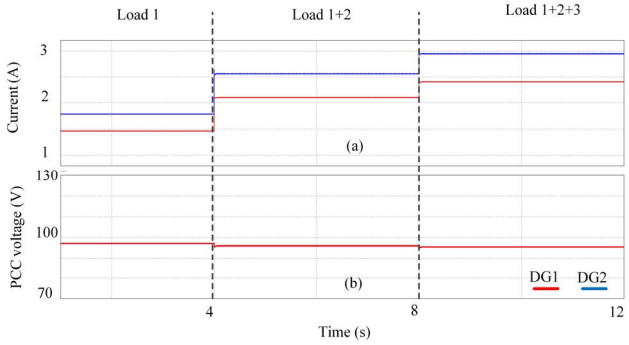

Fig. 7. Conventional droop control: a) Output currents, b) PCC voltage

connecting the load 1, 2 and 3 to the PCC sequentially.

A. Performance with conventional droop control

The performance of the conventional droop control is shown in Fig. 7. Because line resistances are different, the condition for proportional current sharing in (4) is not satisfied. Therefore, from Fig. 7(a), DG 1 with the higher current rating shares the smaller current than DG 2. That means the proportional current sharing is not achieved.

Regarding to the PCC voltage, it decreases below the nominal value of 100V because of the droop characteristic and voltage drop on line resistance, and the degradation becomes severe when the load increases as shown in Fig. 7(b).

B. Performance with proposed control method

The system performance with the proposed control method is shown in Fig. 8 and Fig. 9 shows the output current waveforms, the pu output currents and the AC signal frequencies for the two DGs. From Fig. 8(a) and Fig. 8(b), the accurate current sharing is achieved with a very small AC ripple in spite of different DG current ratings and the load variation. On the other hand, the frequencies of the two DGs converge to the same value in the steady state condition as presented in Fig. 8(c). Because the frequency is related to the pu output current, it deviates from the maximum value of 20Hz and reduces when the load increases.

The PCC voltage waveform and the voltage shift-up are presented in Fig. 9. From Fig. 9, thanks to the voltage shift-up generated from the pu output current of DG, the PCC output

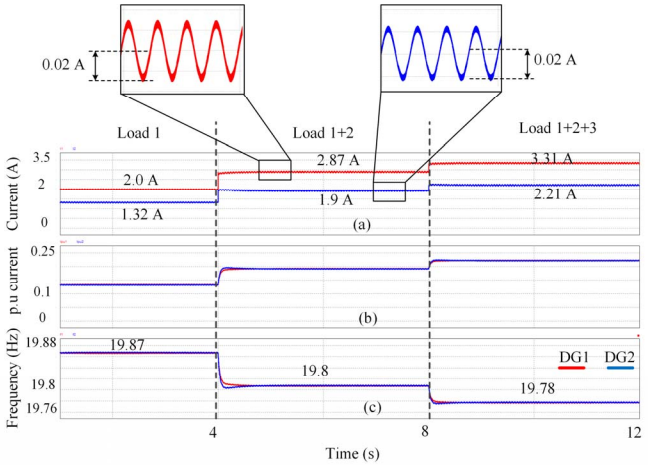

Fig. 8. Proposed control method: a) Output current, b) pu output current, c) AC signal frequency

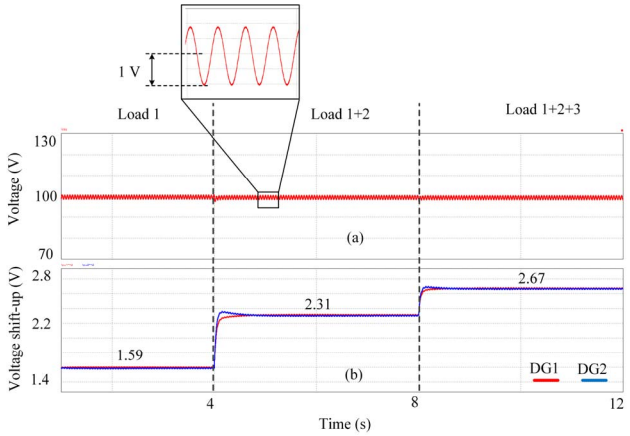

Fig. 9. Proposed control method: a) PCC voltage, b) Voltage shift-up

voltage is regulated to the nominal voltage even if the load increases, and it contains 1.0V sinusoidal ripple because of the injected AC signal.

VI. Conclusion

This paper proposes a current sharing and the PCC voltage restoration approach for LVDC microgrid. In this method, a small AC signal with the frequency, which is proportional to the pu output current of the corresponding DG, is modulated in the output voltage of the DG. By regulating each injected frequency to become the same value, the accurate current sharing is achieved in the steady state. The proposed algorithm can be implemented easily by using the reactive power to regulate the AC signal frequency. In addition, an equivalent voltage shift-up generated from the pu output current is added to the output voltage of DG to restore the PCC voltage to the nominal value. The proposed control method shows the economic efficiency due to it can be implemented in distributed manner without external communication network, and its effectiveness is verified by simulation.

Acknowledgement

This work was partly supported by the National Research

Foundation of Korea Grant funded by the Korean Government (NRF-2015R1D1A1A09058166) and the Korea Institute of Energy Technology Evaluation and Planning (KETEP) and the Ministry of Trade, Industry & Energy (MOTIE) (No. 20174030201490).

REFERENCES

[1] D. Salomonsson, L. Soder, and A. Sannino, "An Adaptive Control System for a DC Microgrid for Data Centers," *IEEE Trans. Ind. Appl.*, vol. 44, no. 6, pp. 1910–1917, Nov. 2008.

[2] K. T. Tan, B. Sivaneasan, X. Y. Peng, and P. L. So, "Control and Operation of a DC Grid-Based Wind Power Generation System in a Microgrid," *IEEE Trans. Energy Convers.*, vol. 31, no. 2, pp. 496–505, Jun. 2016.

[3] H. Wang and J. Huang, "Joint Investment and Operation of Microgrid," *IEEE Trans. Smart Grid*, vol. 8, no. 2, pp. 833–845, Mar. 2017.

[4] Y. Panov, J. Rajagopalan, and F. C. Lee, "Analysis and design of N paralleled DC-DC converters with master-slave current-sharing control," in *Proceedings of APEC 97 - Applied Power Electronics Conference*, 1997, vol. 1, pp. 436–442 vol.1.

[5] L. Guo, Y. Feng, X. Li, C. Wang, and Y. Li, "Stability analysis of a DC microgrid with master-slave control structure," in *2014 IEEE Energy Conversion Congress and Exposition (ECCE)*, 2014, pp. 5682–5689.

[6] D. Chen, L. Xu, and L. Yao, "DC Voltage Variation Based Autonomous Control of DC Microgrids," *IEEE Trans. Power Deliv.*, vol. 28, no. 2, pp. 637–648, Apr. 2013.

[7] Y. Gu, X. Xiang, W. Li, and X. He, "Mode-Adaptive Decentralized Control for Renewable DC Microgrid With Enhanced Reliability and Flexibility," *IEEE Trans. Power Electron.*, vol. 29, no. 9, pp. 5072–5080, Sep. 2014.

[8] T. Dragičević, X. Lu, J. C. Vasquez, and J. M. Guerrero, "DC Microgrids #x2014;Part I: A Review of Control Strategies and Stabilization Techniques," *IEEE Trans. Power Electron.*, vol. 31, no. 7, pp. 4876–4891, Jul. 2016.

[9] P. Wang, X. Lu, X. Yang, W. Wang, and D. Xu, "An Improved Distributed Secondary Control Method for DC Microgrids With Enhanced Dynamic Current Sharing Performance," *IEEE Trans. Power Electron.*, vol. 31, no. 9, pp. 6658–6673, Sep. 2016.

[10] P. H. Huang, P. C. Liu, W. Xiao, and M. S. El Moursi, "A Novel Droop-Based Average Voltage Sharing Control Strategy for DC Microgrids," *IEEE Trans. Smart Grid*, vol. 6, no. 3, pp. 1096–1106, 2015.

[11] X. Lu, J. M. Guerrero, K. Sun, and J. C. Vasquez, "An Improved Droop Control Method for DC Microgrids Based on Low Bandwidth Communication With DC Bus Voltage Restoration and Enhanced Current Sharing Accuracy," *IEEE Trans. Power Electron.*, vol. 29, no. 4, pp. 1800–1812, 2014.

[12] S. Anand, B. G. Fernandes, and J. Guerrero, "Distributed Control to Ensure Proportional Load Sharing and Improve Voltage Regulation in Low-Voltage DC Microgrids," *IEEE Trans. Power Electron.*, vol. 28, no. 4, pp. 1900–1913, 2013.

[13] V. Nasirian, A. Davoudi, F. L. Lewis, and J. M. Guerrero, "Distributed Adaptive Droop Control for DC Distribution Systems," *IEEE Trans. Energy Convers.*, vol. 29, no. 4, pp. 944–956, 2014.

[14] M. Angjelichinoski, Č. Stefanović, P. Popovski, H. Liu, P. C. Loh, and F. Blaabjerg, "Multiuser Communication Through Power Talk in DC MicroGrids," *IEEE J. Sel. Areas Commun.*, vol. 34, no. 7, pp. 2006–2021, Jul. 2016.

[15] A. Tuladhar, H. Jin, T. Unger, and K. Mauch, "Parallel operation of single phase inverter modules with no control interconnections," in *Proceedings of APEC 97 - Applied Power Electronics Conference*, 1997, vol. 1, pp. 94–100 vol.1.

[16] A. Tuladhar and H. Jin, "A novel control technique to operate DC/DC converters in parallel with no control interconnections," in *PESC 98 Record. 29th Annual IEEE Power Electronics Specialists Conference (Cat. No.98CH36196)*, 1998, vol. 1, pp. 892–898 vol.1.

[17] S. Peyghami, H. Mokhtari, P. C. Loh, P. Davari, and F. Blaabjerg, "Distributed Primary and Secondary Power Sharing in a Droop-Controlled LVDC Microgrid with Merged AC and DC Characteristics," *IEEE Trans. Smart Grid*, vol. PP, no. 99, p. 1, 2016.

[18] S. Peyghami, H. Mokhtari, and F. Blaabjerg, "Decentralized Load Sharing in a Low-Voltage Direct Current Microgrid With an Adaptive Droop Approach Based on a Superimposed Frequency," *IEEE J. Emerg. Sel. Top. Power Electron.*, vol. 5, no. 3, pp. 1205–1215, Sep. 2017.

[19] S. Peyghami, P. Davari, H. Mokhtari, P. C. Loh, and F. Blaabjerg, "Synchronverter-Enabled DC Power Sharing Approach for LVDC Microgrids," *IEEE Trans. Power Electron.*, vol. 32, no. 10, pp. 8089–8099, Oct. 2017.

[20] J. M. Guerrero, L. Hang, and J. Uceda, "Control of Distributed Uninterruptible Power Supply Systems," *IEEE Trans. Ind. Electron.*, vol. 55, no. 8, pp. 2845–2859, Aug. 2008.